

## PECTORALIS MUSCLE PERFORMANCE DURING ASCENDING AND SLOW LEVEL FLIGHT IN MALLARDS (*ANAS PLATYRHYNCHOS*)

MICHAEL R. WILLIAMSON<sup>1</sup>, KENNETH P. DIAL<sup>2</sup> AND ANDREW A. BIEWENER<sup>1,\*</sup>

<sup>1</sup>Concord Field Station, Museum of Comparative Zoology, Department of Organismic and Evolutionary Biology, Harvard University, Old Causeway Road, Bedford, MA 01730, USA and <sup>2</sup>Division of Biological Sciences, University of Montana, Missoula, MT 59812, USA

\*Author for correspondence (e-mail: abiewener@oeb.harvard.edu)

Accepted 13 November 2000; published on WWW 15 January 2001

### Summary

*In vivo* measurements of pectoralis muscle length change and force production were obtained using sonomicrometry and delto-pectoral bone strain recordings during ascending and slow level flight in mallards (*Anas platyrhynchos*). These measurements provide a description of the force/length properties of the pectoralis under dynamic conditions during two discrete flight behaviors and allow an examination of the effects of differences in body size and morphology on pectoralis performance by comparing the results with those of a recent similar study of slow level flight in pigeons (*Columbia livia*). In the present study, the mallard pectoralis showed a distinct pattern of active lengthening during the upstroke. This probably enhances the rate of force generation and the magnitude of the force generated and, thus, the amount of work and power produced during the downstroke. The power output of the pectoralis averaged 17.0 W kg<sup>-1</sup> body mass

(131 W kg<sup>-1</sup> muscle mass) during slow level flight (3 m s<sup>-1</sup>) and 23.3 W kg<sup>-1</sup> body mass (174 W kg<sup>-1</sup> muscle mass) during ascending flight. This increase in power was achieved principally via an increase in muscle strain (29% versus 36%), rather than an increase in peak force (107 N versus 113 N) or cycle frequency (8.4 Hz versus 8.9 Hz). Body-mass-specific power output of mallards during slow level flight (17.0 W kg<sup>-1</sup>), measured in terms of pectoralis mechanical power, was similar to that measured recently in pigeons (16.1 W kg<sup>-1</sup>). Mallards compensate for their greater body mass and proportionately smaller wing area and pectoralis muscle volume by operating with a high myofibrillar stress to elevate mechanical power output.

Key words: pectoralis muscle, muscle, mallard, *Anas platyrhynchos*, bone strain, flight, strain, power output, work loop.

### Introduction

The mechanical power requirements of avian flight are of interest both in terms of whole-animal performance and in terms of the neural and musculoskeletal processes underlying that performance. Prior investigations of avian flight, however, have been unable to reconcile predictions of aerodynamic power with measurements or estimates of muscle mechanical power. Previous estimates of mechanical power have been based largely on quasi-steady aerodynamic theory and observations of flight kinematics (e.g. Pennycuik, 1968; Norberg, 1990) in relation to assumed limits of vertebrate muscle function (Weis-Fogh and Alexander, 1977). A potential limitation of these models is that they do not account for unsteady airflow over the flapping wing, which has been shown to be central to mechanisms of lift generation in insect flight (e.g. Dickinson et al., 1999; Willmott and Ellington, 1997; Weis-Fogh, 1973) and which may also be important in avian flight. In addition, such analyses do not account for variation in flight behavior or body form. Vortex-based theories of aerodynamic power designed to deal with these issues (Rayner,

1979), however, have also tended to overestimate considerably the power required of birds during slow level flight (Spedding et al., 1984; Spedding, 1986).

Most recently, the power requirements of a swallow have been assessed by direct measurements of the vertical motion of the bird flying in a wind tunnel (Pennycuik et al., 2000) combined with previous theory (Pennycuik, 1968; Pennycuik, 1989) for profile and body drag and the lift distribution acting on a fixed-form, fully extended wing during the downstroke. Although this study ignored horizontal accelerations of the animal in the wind tunnel and the long-axis rotational energy of the wing (produced by the pectoralis at the shoulder), which would require additional power, these measurements also resulted in estimates of mechanical power twice those predicted by theory. Significant differences therefore continue to exist between empirical assessments and theoretical predictions of the power requirements for avian flight.

Because of the uncertainties underlying assumptions made

by aerodynamic models of avian flight, we have favored the use of direct recordings of pectoralis force made *in vivo* during flight to calculate mechanical power (Biewener et al., 1992; Dial and Biewener, 1993; Dial et al., 1997). The pectoralis produces most of the power required for lift generation in birds (Dial, 1992); therefore, measurements of its mechanical power output can provide a reliable estimate of the total aerodynamic power required for flight. Previous studies have used *in vivo* pectoralis force recordings combined with kinematic estimates of muscle shortening to calculate mechanical power output during flight in starlings (*Sturnus vulgaris*; Biewener et al., 1992), pigeons (*Columbia livia*; Dial and Biewener, 1993) and magpies (*Pica pica*; Dial et al., 1997). The results of these studies suggest that classical aerodynamic predictions overestimate the actual power requirements of bird flight and that differences in flight performance or behavior may be achieved by smaller changes in mechanical power than was previously thought. More recently, Biewener et al. (Biewener et al., 1998) combined *in vivo* measurements of pectoralis force with direct sonometric recordings of fascicle length changes in a study of level flight in pigeons (*Columbia livia*). These recordings confirmed the general magnitude of muscle strain estimated previously from wing kinematics, but indicated less active lengthening late in the upstroke and more substantial force decline during the shortening phase of the muscle's contraction. As a result, modest but significant differences in the dynamic force/length behavior of the muscle were revealed by the combined *in vivo* force and sonomicrometry recordings.

The purpose of the present study is to build upon the results obtained for pigeons by examining the force/length behavior of the pectoralis muscle in mallards (*Anas platyrhynchos*) to assess its mechanical power output during both ascending and slow level flight. We anticipate that the general patterns of pectoralis force/length behavior during flight in the mallards will be similar to those previously observed in other species. In addition, we hypothesize that mechanical power output will be greater during ascending than during level flight as a result of concomitant increases in muscle force, strain and wingbeat frequency. Finally, we hypothesize that the mallard's greater size will require it to produce greater absolute muscle power than the pigeon, but that the mass-specific mechanical power output of both species will be similar under comparable conditions of flight behavior.

## Materials and methods

### *Animals, training and definition of flight modes*

Four mallards (body mass range 0.97–1.06 kg; Table 1) were purchased from a licensed game farm (Ducks and Ducks Game Farm, Trumann, AR, USA), housed in heated enclosures (6 m×2 m×3 m) and provided with commercial bird feed (Muenster Milling Co.) and water *ad libitum*. Prior to data collection, each of the birds was flown in the experimental area until it demonstrated an ability to fly the desired course for flight recordings. This involved taking off from the ground at a steep trajectory ( $\geq 60^\circ$ ), clearing a barrier (1.22–2 m) and flying up to 8 m down a narrow (1.4 m) corridor before landing on the ground (see Fig. 2B). During the training and flight recordings, the animals were handled as little as possible to avoid acclimation to human contact and the possible reduction of their burst take-off escape response.

To examine the mechanical performance of the pectoralis under varying flight conditions, we defined two flight modes for comparison. Ascent was defined as the portion of the flight sequence that began at least two cycles after lift-off from the ground and was maintained at a steady angle and rate of climb for a minimum of four wingbeats. This was the period during which the birds achieved their steepest ascent prior to clearing the barrier. This burst take-off behavior was considered to be indicative of maximal unladen flight performance in these animals. Slow level flight was defined as that portion of the flight during which the flight trajectory was horizontal for several (at least four) wingbeats. Level flights were typically obtained either as the bird flew over the barrier following hand-release from an elevated position or as the bird flew down the corridor following take-off from the ground and clearance of the barrier. Forward airspeed during slow level flight was approximately  $3 \text{ m s}^{-1}$ , as determined from timed flight positions obtained from high-speed video measurements (see below).

### *Transducer implantation*

Anesthesia for surgical implantation of transducers was induced by an intravenous injection of sodium pentobarbital ( $20 \text{ mg kg}^{-1}$ ) and maintained during the procedure with intermittent administration of methoxyflurane gas (Metofane) *via* a mask. The feathers were removed from small areas on the dorsal midline between the scapulae, on the ventral side of one pectoralis and on the ipsilateral shoulder; a single incision (15–40 mm) was made at each site.

Table 1. *Pectoralis and wing morphology of experimental animals*

Animal	Body mass (kg)	Pectoralis mass (kg)	Fascicle length (mm)	Myofibrillar area (cm <sup>2</sup> )	Wing span (cm)	Wing area (cm <sup>2</sup> )	Wing loading (N m <sup>-2</sup> )
1	0.97	0.081	71.0	6.46	84.6	818	116.3
2	1.03	0.053	70.9	4.23	88.0	1097	92.1
3	0.92	0.068	72.7	5.29	85.2	853	105.8
4	1.06	0.067	64.2	5.91	87.0	938	110.9
Mean	0.995	0.067	69.7	5.47	86.2	927	106.3
S.D.	0.062	0.012	3.76	0.96	1.57	124	10.4

Through the shoulder incision, the deltoid was reflected to expose the dorsal surface of the delto-pectoral crest (DPC) of the humerus. In previous studies (Biewener et al., 1992; Biewener et al., 1998; Dial and Biewener, 1993; Dial et al., 1997), dorsal DPC strain has been used to quantify *in vivo* pectoralis force development. This approach relies on the assumption that the pectoralis generates a tensile strain in the dorsal aspect of the DPC along a principal axis at approximately 90° to the humeral shaft when it contracts to pull down against its ventral insertion (Dial and Biewener, 1993). Using a metal foil strain gauge bonded to the surface of the DPC along this axis, bone strains produced by the pectoralis can be calibrated to force (see below; Biewener et al., 1998; Biewener et al., 1992; Dial and Biewener, 1993; Dial et al., 1997). Accordingly, the surface of the bone was scraped gently with a periosteal elevator and/or a scalpel blade to remove the periosteum, then cleaned and dried with a sterile swab dipped in anhydrous ethyl ether, so that a single-element (type FLA-1-11, Tokyo Sokki Kenkyujo, Japan) or rosette (FRA-1-11) strain gauge could be bonded to the DPC with cyanoacrylate adhesive. The three-element rosette strain gauge was used on one bird (mallard 3) to characterize the pattern and orientation of principal strains on the dorsal DPC. Leads from the gauge were passed deep to the deltoid and subcutaneously to the dorsal midline incision.

Through the ventral incision, sonomicrometry transducers ('crystals'; Triton P/N SL 5-2 or Sonometrics 2 mm 36 AWG SS) were implanted into an area of the sternobrachialis portion of the pectoralis in which the muscle's fascicles originate on the sternum and insert directly onto the ventral aspect of the DPC. Two small spaces (3 mm across, 6 mm deep) between muscle fascicles were made approximately 15 mm apart along a single fascicular element using small, sharp-pointed scissors; the sonomicrometry crystals were inserted into these spaces. These crystals measure the distance between them by recording the transit time of an ultrasonic acoustic signal transmitted from one to the other, given an estimate of the speed of sound in the muscle tissue (1540 m s<sup>-1</sup>; Goldman and Heuter, 1956). Assuming that the length changes between the crystals are representative of the fascicle and that the fascicle length changes measured are characteristic of those throughout the muscle, these recordings can be used to estimate whole-muscle length changes *in vivo* (Griffiths, 1987). After insertion of the crystals, the openings in the muscle fascia were closed, and the leads were secured to the fascia with 4-0 silk suture. To maintain orientation, the Triton crystals used in one animal (mallard 1) were mounted with epoxy adhesive onto small loops of 18-gauge surgical wire, which were sutured to the muscle fascia.

Two bipolar electromyographic (EMG) electrodes (0.1 mm diameter, 99.9% silver, enamel-insulated wire; California Fine Wire; 0.5 mm tip exposure and 1 mm spacing) were implanted in the pectoralis muscle adjacent to the sonomicrometry crystals using a 22-gauge hypodermic needle. These electrodes were used to verify the timing of local muscle activation relative to fascicle shortening and force production. EMG leads

were sutured to the muscle fascia with 4-0 silk at two places near the point of insertion.

Leads from each of the implanted transducers were passed subcutaneously to a custom-designed connector (Microtech GF-6) supported on an epoxy base. This connector was secured to the dorsal midline of the body by suturing the base to the intervertebral ligaments and closing the skin around it. All incisions were kept moist during surgery and sutured with 3-0 silk when each procedure had been completed. Animals were allowed to recover from surgery overnight prior to flight recordings.

#### Flight recordings

Experimental recordings of pectoralis force production, fascicle length change and EMG activity were carried out 1–2 days following surgery. All transducers were connected to their respective amplifiers *via* a lightweight shielded cable (Cooner; model NMUF4/30-4046SJ, weighing 0.32 N m<sup>-1</sup> and a maximum of approximately 0.69 N in total), which was grounded to the skin of the bird and taped to its back to reduce mechanical stress at the end of the cable. EMG signals from the pectoralis were amplified (2000×) and filtered (100–3000 Hz half-amplitude band-pass, 60 Hz notch filter) using Grass P511 amplifiers. Bone strain signals from the strain gauges were amplified (2000×) using a bridge amplifier (Vishay; model 2150). All sonomicrometry data were processed and amplified by a Triton sonomicrometer (model 120.2) that imposed a 5 ms delay (Marsh et al., 1992), which was corrected in subsequent analyses. In addition, signal offsets due to the transmission through the epoxy lens of the crystals were determined and corrected (0.74 mm for Triton crystals; 0.82 mm for Sonometrics). All signals were recorded on LabVIEW 4.0 (mallard 1) or Axoscope 7.0 software, then filtered and analyzed in MS Excel 98 and IGOR 3.1 software.

Video recordings of each pre-surgical and implanted flight were made to calculate whole-body climbing power, to verify normal flight behavior following surgery and to provide a record of the specific flight behavior for each flight sequence. The initial experiment (mallard 1) was recorded from lateral and posterior views using Sony Hi8 (CCD-TRV81) and digital (DCR-VX1000) video cameras at 60 Hz. Later experiments (mallards 2, 3 and 4) were recorded from a lateral perspective at 250 Hz using a Redlake digital camera (PCI 500). These video sequences were analyzed using NIH Image 1.60 and Videopoint software, respectively. Whole-body climbing power ( $P$ ) was calculated as the sum of the rates of change of potential and kinetic energy using the following equation:

$$P = (mgh + \frac{1}{2}m\Delta v^2)/t,$$

where  $m$  is body mass,  $g$  is the acceleration due to gravity,  $h$  is the height change of the bird's center of mass,  $\Delta v$  is the change in velocity measured along the animal's flight path over a given interval of its climb and  $t$  is time.

Following the completion of flight recordings, the birds were killed (sodium pentobarbital, 65 mg kg<sup>-1</sup> intravenously) to carry out force calibrations and obtain morphological measurements.

### Calibrations and morphological measurements

To calibrate DPC strain recordings to pectoralis force, a series of 'pull' calibrations was carried out *post-mortem* by holding the humerus fixed and pulling on the pectoralis just distal to its ventral insertion in the direction of the fibers with heavy (0 gauge or larger) silk suture attached to a calibrated force transducer (Kistler; model 9203). Although this calibration routine was similar to that used in previous studies utilizing this method of force measurement (Biewener et al., 1992; Biewener et al., 1998; Dial and Biewener, 1993; Dial et al., 1997), it has potential sources of error. First, the calibration is carried out under static conditions with the wing held in a fixed position. In addition, the results may be sensitive to differences in gauge placement, wing position and the orientation of the applied force. The issue of gauge placement may be more critical in mallards than in previously studied species because of the mallard's broader pectoral insertion and less prominent DPC. Because of this morphology, more complex, and potentially variable, patterns of bone strain may occur locally at the site of gauge attachment. Considerable care was taken to minimize these potential sources of error, and the potential for strain variation was examined by recording the principal strain distribution in one animal (mallard 3).

After DPC strain calibration, the following morphological measurements were obtained: pectoralis mass, mean fascicle length and pinnation angle (based on measurements of 10–20 fascicles evenly distributed throughout the muscle, using digital calipers), pectoralis moment arm ( $r_{\text{pect}}$ ) at the shoulder, wing span and wing area (integrated from a digital image of a wing trace using NIH Image 1.60; Table 1). Fascicle length changes of the pectoralis were calculated from the *in vivo* fractional length changes measured between the crystals ( $\Delta L/L_{\text{rest}}$ , where  $L_{\text{rest}}$  is the resting length measured between the crystals at the end of a flight and confirmed *post-mortem*). Fractional length change measured between the crystals was multiplied by the muscle's mean fascicle length to obtain the mean fascicle length change of the muscle as a whole. This assumes that all active fascicles contract with equal fractional length change. Muscle cross-sectional area was calculated according to Calow and Alexander (Calow and Alexander, 1973) and corrected to myofibrillar area (60% of total area; Rosser and George, 1986). Intramuscular stress was calculated from the pectoralis force and myofibrillar area. The centroid of wing area for two birds (mallards 2 and 3) was determined and used to approximate the center of aerodynamic pressure. The distance from the shoulder to this estimated center of pressure is equal to the moment arm of the wing ( $r_{\text{wing}}$ ), which

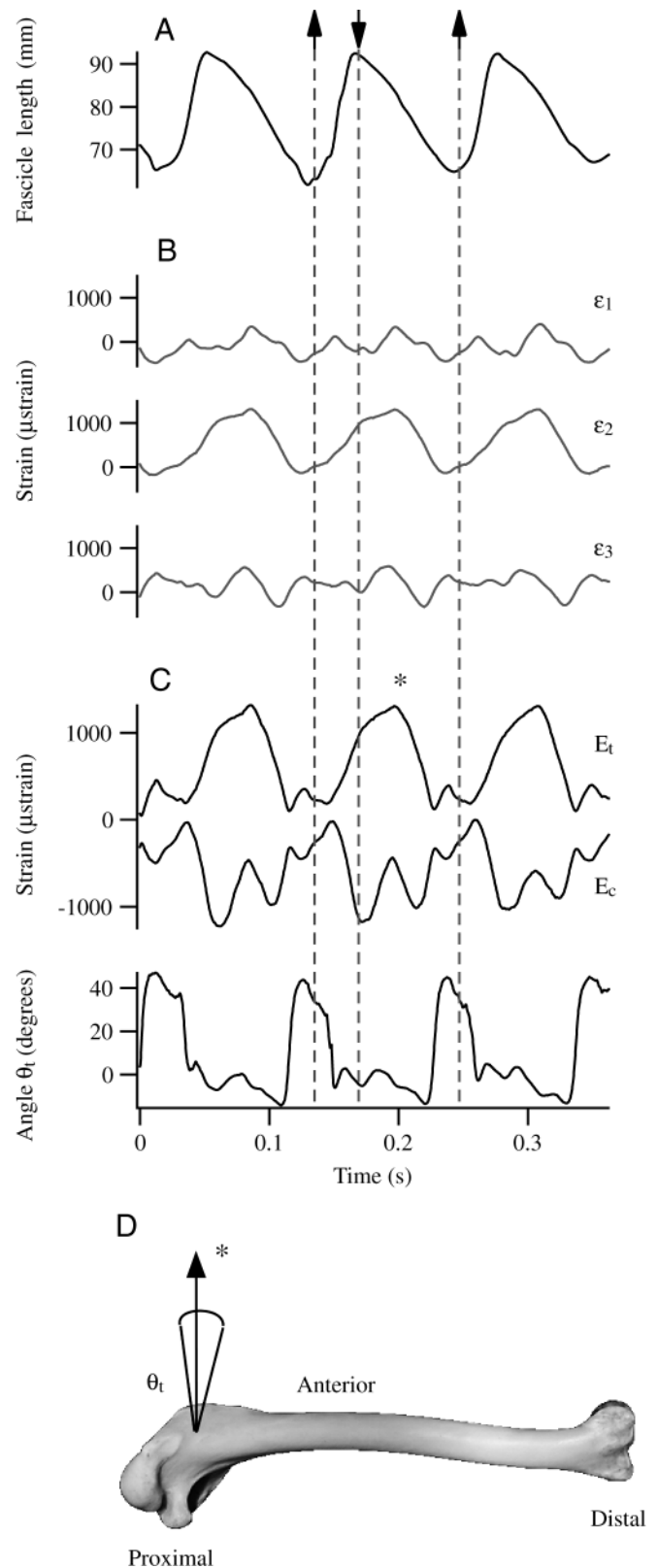


Fig. 1. Simultaneous traces of (A) pectoralis muscle length change and (B) rosette strain gauge recordings ( $\epsilon_1$ ,  $\epsilon_2$  and  $\epsilon_3$ ) from the deltopectoral crest (DPC) in three wingbeat cycles during level flight. Dashed lines and arrows indicate upstroke and downstroke transitions. (C) Principal tensile ( $E_t$ ) and compressive ( $E_c$ ) strains derived from signals in B, and a plot of the angle of orientation ( $\theta_t$ ) of the principal tensile strain. Note that  $0^\circ$  is perpendicular to the long axis of the humerus. (D) Dorsal view of the left humerus, indicating the angle ( $\theta_t$ ) of principal tensile strain on the DPC during pectoralis force development. Orientation varied from  $+1^\circ$  to  $-21^\circ$  during this period. An asterisk denotes peak tensile strain, as in C. The vector represents the mean orientation of peak strain at  $-6^\circ$ .

was then used to estimate the mechanical advantage of the pectoralis ( $r_{\text{pect}}/r_{\text{wing}}$ ) for depressing the wing. These measurements were also obtained for the wings of two white carneau pigeons (*Columbia livia*), similar in size to the silver king pigeons used by Biewener et al. (Biewener et al., 1998), for the purpose of comparing pectoralis mechanical advantage between the two species.

Values are presented as means  $\pm$  s.d.

## Results

### Delto-pectoral crest strain pattern

The raw strains ( $\epsilon_1$ ,  $\epsilon_2$ ,  $\epsilon_3$ ) recorded from the rosette strain gauge attached to the DPC of mallard 3 are presented in Fig. 1B, together with the principal tensile and compressive strains ( $E_t$ ,  $E_c$ ) and the orientation ( $\theta_t$ ) of principal tensile strain derived from them (Fig. 1C). Sonomicrometry recordings of pectoralis length change are shown (Fig. 1A) for the same three wingbeat cycles. During the downstroke, as strain increases because of tension applied by the pectoralis, the orientation of the principal tensile DPC strain varied on average from  $1^\circ$  proximal to  $21^\circ$  distal to an axis perpendicular to the long axis of the humerus (Fig. 1D;  $N=34$ ). At peak strain (indicated by an asterisk in Fig. 1C,D and the vector in Fig. 1D), the orientation of principal tension averaged  $-6\pm 3^\circ$  ( $N=34$ ). The large fluctuations in principal strain orientation that occur during the downstroke-to-upstroke transition probably reflect changes in the distribution of smaller forces transmitted to the DPC by the wing elevators after the cessation of pectoralis activity (Fig. 1C). The similarity in the magnitude and timing of  $\epsilon_2$  and  $E_t$ , as well as the narrow range of principal tensile strain orientation, combined with similar results from previous studies, confirm the reliability of our subsequent use of a single-element strain gauge aligned to this perpendicular ( $\epsilon_2$ ) axis to measure DPC strains produced by the pectoralis in the three other mallards.

### Pectoralis length change, force and activation

*In vivo* recordings of pectoralis length change, force production and activation showed patterns of oscillation expected for the muscle's function to produce lift during the downstroke (Figs 2, 3). During slow level flight, the pectoralis lengthened to  $121.5\pm 4.1\%$  of its resting length (determined from the muscle's length recorded when the birds were resting on the ground between trials) and shortened to  $92.2\pm 2.5\%$  of its resting length, resulting in an overall strain of  $29.3\pm 2.4\%$  (Fig. 2; Table 2;  $N=4$ ). The trajectory of this strain was asymmetrical, with the shortening phase of the cycle (downstroke) occupying  $69.0\pm 2.5\%$  of the cycle period (Figs 3, 4;  $N=4$ ). Cycle frequency during level flight was  $8.4\pm 0.3$  Hz, resulting in a mean shortening velocity of  $3.7\pm 0.4$  lengths  $s^{-1}$  over the entire period of the downstroke (Tables 2, 3;  $N=4$ ).

The recorded EMG activity displayed a pattern that was consistent with changes in muscle length and force development (Fig. 2). During level flight, neural activation of

the muscle began midway through the lengthening phase, preceding the start of shortening by  $17\pm 5$  ms, and ceased midway through the shortening phase,  $32\pm 5$  ms after the onset of shortening (Figs 3, 4;  $N=4$ ). Correspondingly, neural activation preceded the onset of force production by  $7\pm 5$  ms and ended  $21\pm 5$  ms before the muscle reached peak force (Figs 3, 4;  $N=4$ ).

Because of the timing of neural activation, force onset during slow level flight occurred  $9\pm 6$  ms prior to the start of

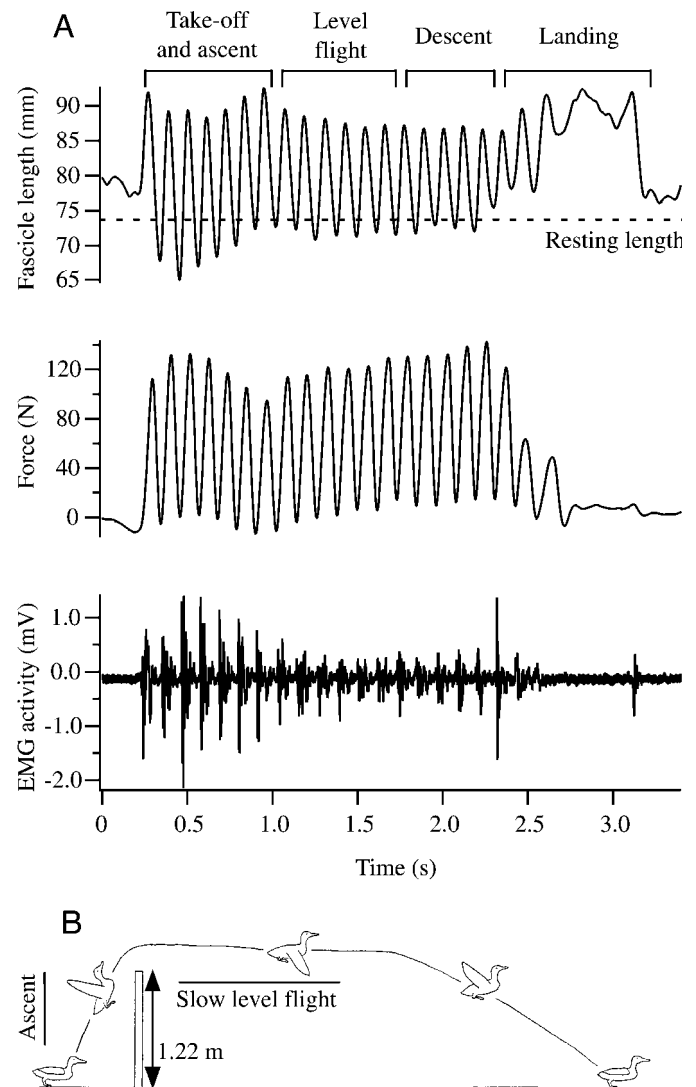


Fig. 2. *In vivo* recordings of pectoralis length change calibrated from sonomicrometry data, together with simultaneous recordings of pectoralis force calibrated from strains on the delto-pectoral crest and electromyographic (EMG) recordings from the pectoralis (A). The dashed line indicates resting fascicle length, as determined from the fascicle length recorded when the bird was resting on the ground between trials. During this sequence, the bird took off and ascended over a barrier, flew level down a hallway, then descended and landed several meters away. Most flight sequences followed a similar pattern, and the data for ascent and level flight were drawn from the portions of the flight indicated. (B) Schematic drawing of a representative flight sequence.

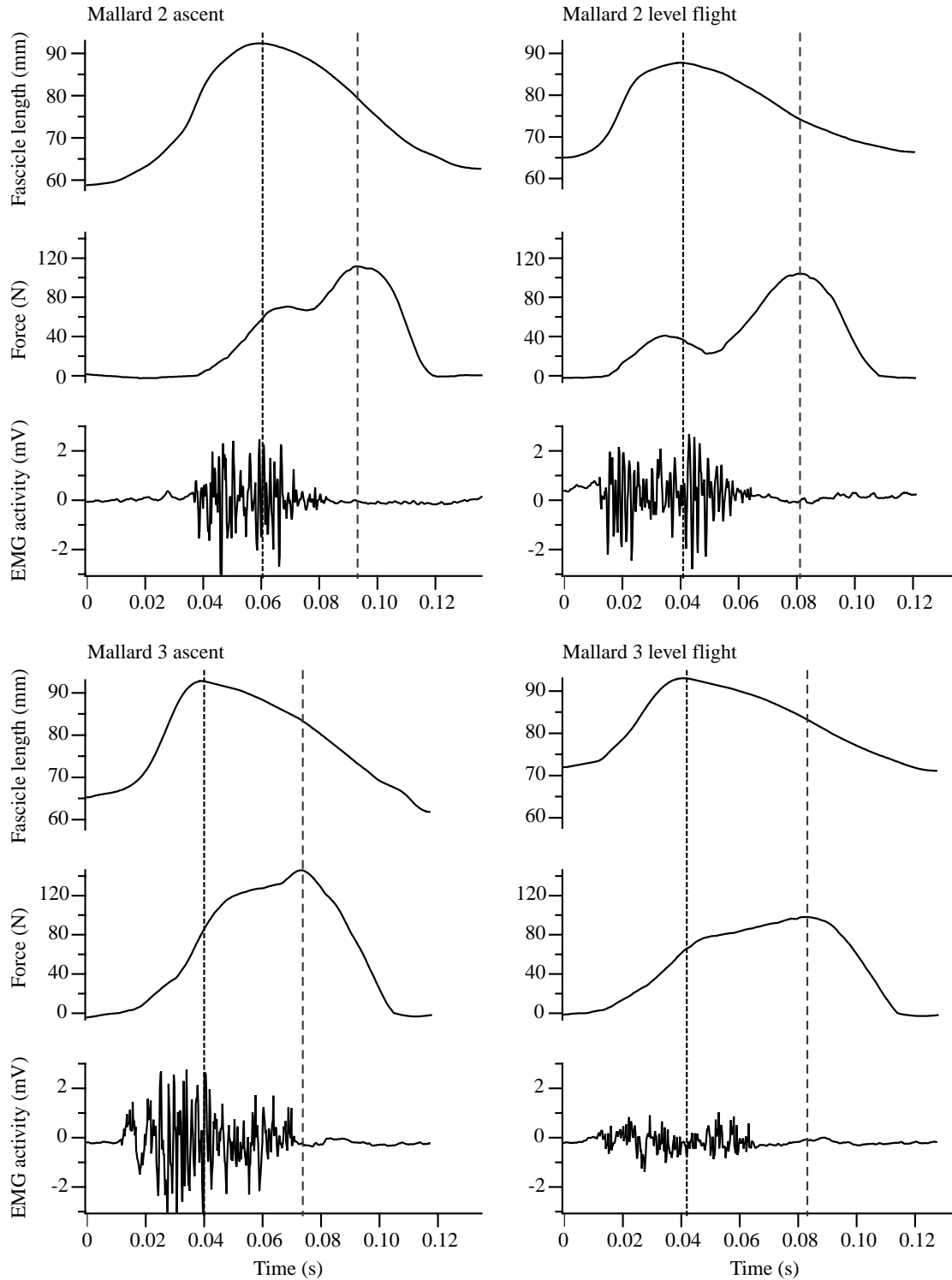


Fig. 3. Expanded wingbeat cycles from mallards 2 and 3 showing the relative timing of pectoralis length change, force development and neural (electromyographic, EMG) activation within a cycle, as well as differences in the magnitude and timing of these variables between ascent and slow level flight. The short-dashed line marks peak fascicle length, while the long-dashed line marks peak force. The bimodal force trace for mallard 2 is probably an artifact (see text).

the downstroke. This resulted in a distinct pattern of active lengthening of the mallard pectoralis during the upstroke (Figs 3, 4;  $N=4$ ). Force development during level flight peaked

at  $107.5 \pm 10.6$  N (Table 2;  $N=4$ ) approximately two-thirds of the way through the downstroke,  $54 \pm 6$  ms after the start of shortening, and fell to zero just prior to the muscle

Table 2. Summary of mallard pectoralis muscle performance during ascending and slow level flight

Animal	Behavior	N	Frequency (Hz)	Downstroke duration (% cycle)	Muscle lengthening (% rest)	Muscle shortening (% rest)	Peak force (N)	Work (mJ)	Total power (W)	Muscle-specific power (W kg <sup>-1</sup> )	Body-mass-specific power (W kg <sup>-1</sup> )
1	AS	6	8.48±0.51	66.84±3.98	22.63±1.61	-12.19±2.73	118.18±12.46	1651.81±178.47	27.98±3.25	172.73±20.09	28.85±3.36
	LF	12	8.08±1.34	65.84±5.07	20.35±2.04	-7.53±2.41	108.23±32.90	974.94±296.15	15.89±5.92	98.08±36.55	16.38±6.10
2	AS	15	8.84±0.88	66.14±3.57	26.85±1.67	-9.65±3.59	84.91±15.37	1331.89±482.99	23.08±6.62	217.76±62.48	22.41±6.43
	LF	15	8.70±0.54	68.24±3.19	19.26±3.68	-10.80±1.59	101.66±12.23	1207.84±271.06	20.99±4.67	198.00±44.01	20.38±4.53
3	AS	18	9.12±0.35	70.40±3.09	20.20±0.80	-15.75±2.92	145.64±6.36	1082.20±355.99	19.70±6.23	145.05±45.89	21.41±6.77
	LF	19	8.22±0.29	70.18±2.40	18.86±1.83	-8.05±1.44	121.99±11.30	792.96±196.62	12.99±3.00	95.57±22.08	14.12±3.26
4	AS	8	9.26±0.27	64.77±2.37	30.67±7.89	-5.27±4.15	101.36±16.92	1184.92±270.30	21.91±4.84	161.10±35.61	20.67±4.57
	LF	16	8.59±0.71	71.72±4.99	27.57±5.46	-4.76±4.19	97.93±17.41	1041.65±246.54	17.93±4.61	131.84±33.93	16.92±4.35
Mean	AS	4	8.93±0.34	67.04±2.40	25.09±4.63	-10.72±4.41	112.52±25.92	1312.71±248.21	23.17±3.50	174.16±31.20	23.34±3.75
	LF	4	8.40±0.29	69.00±2.54	21.51±4.09	-7.79±2.47	107.45±10.59	1004.35±171.61	16.95±3.37	130.87±47.71	16.95±2.59

All values are presented as means ± s.d.  
AS, ascending flight; LF, slow level flight.

Table 3. Comparison of mallard versus pigeon morphology and pectoralis muscle performance in slow level flight

Animal	Body mass (kg)	Pectoralis mass (kg)	Fascicle length (mm)	Wing loading (N m <sup>-2</sup> )	Wingbeat frequency (Hz)	Muscle strain (% rest)	Shortening velocity (muscle lengths s <sup>-1</sup> )	Peak force (N)	Pectoralis work (mJ)	Pectoralis power (W)	Muscle-specific power (W kg <sup>-1</sup> )	Body-mass-specific power (W kg <sup>-1</sup> )
Mallard	0.995±0.062	0.135±0.023	69.7±3.8	106.3±10.4	8.40±0.29	29.3±2.4	3.66±0.44	107.5±10.6	1004.4±171.6	16.95±3.37	130.9±47.7	16.95±2.59
Pigeon	0.649±0.032	0.116±0.007	55.0±5.0	75.0±7.9	8.70±0.26	32.8±8.0	5.13±1.30	47.3±6.8	614.8±211.9	10.44±2.87	90.0±24.7	16.08±4.61

Pigeon values are taken from Biewener et al., 1998.  
All values are presented as means ± s.d.

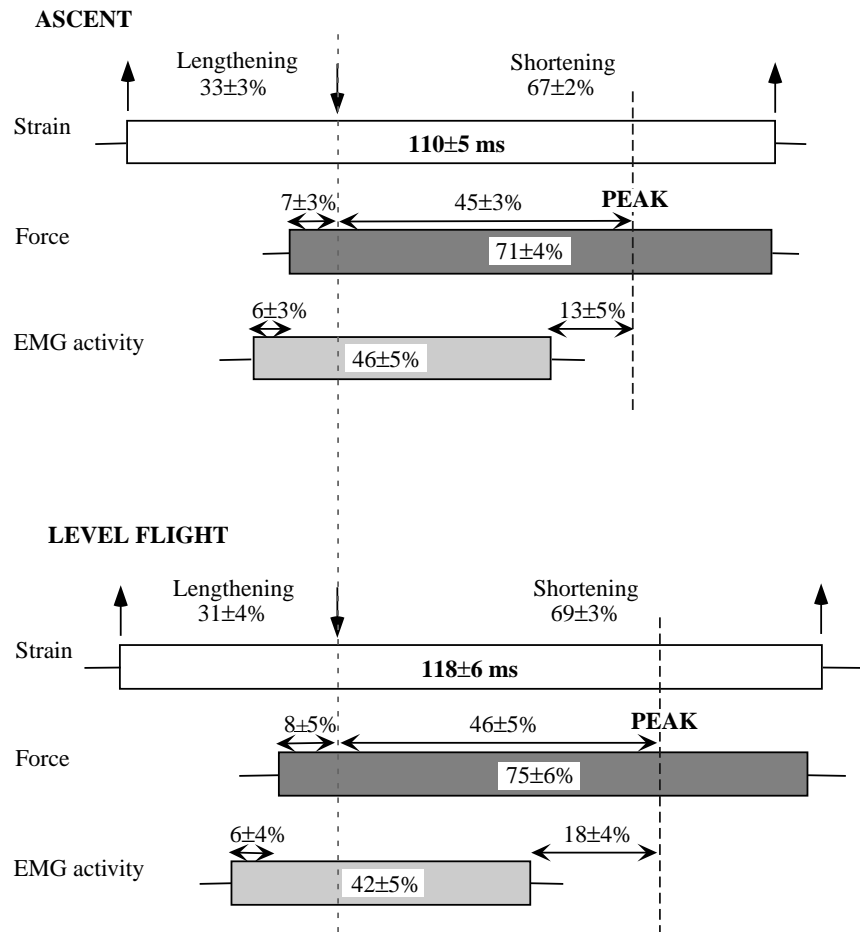


Fig. 4. Diagram showing the timing (mean  $\pm$  S.D.,  $N=4$ ) of pectoralis force production and electromyographic (EMG) activity relative to that of the fascicle length change. Values in bold type on the strain bars are cycle durations; other values are indicated as a percentage of the cycle period. Vertical arrows and the gray dashed line mark transitions between the shortening and lengthening phases. The black dashed line marks peak force.

subsequently being relengthened (Figs 3, 4;  $N=4$ ). The bimodal force trace seen in the recording for mallard 2 during the downstroke (Fig. 3) probably reflects variation in strain pattern generated by the pectoralis during the downstroke and/or slight misalignment of the DPC strain gauge relative to the principal strain axis. This pattern was much less evident in mallards 1 and 4, and was not observed in mallard 3. Given the similarity between the  $\epsilon_2$  gauge trace and the derived principal strain for mallard 3, we believe that the pattern recorded for mallard 3 is most representative of the actual force profile produced by the pectoralis in these birds (Fig. 1). We present both patterns to show the extremes of variation in force-calibrated strain signals recorded.

During ascending flight, pectoralis strain increased to  $35.8 \pm 0.7\%$  as the pectoralis lengthened to  $125.1 \pm 4.6\%$  and shortened to  $89.3 \pm 4.4\%$  of its resting length (Figs 2–4; Table 2;  $N=4$ ). The asymmetry of the length trajectory during ascent was similar to that in level flight, with the shortening phase accounting for  $67.0 \pm 2.4\%$  of the cycle period (Figs 3, 4;  $N=4$ ). Cycle frequency also increased to  $8.9 \pm 0.3$  Hz. Consequently, as a result of the increase in strain and frequency, a significantly greater shortening velocity of  $4.9 \pm 0.3$  lengths  $s^{-1}$  was achieved during ascent (Table 2;  $N=4$ ).

In general, larger EMG amplitudes and forces were observed during ascending than during slow level flight (Figs 1, 3).

When normalized to cycle period, the timing of neural activation and force onset and offset were unchanged between the two flight modes (Fig. 4). During ascending flight, neural activation preceded force production by  $7 \pm 3$  ms, and the onset of force production preceded the start of muscle shortening by  $8 \pm 3$  ms (Fig. 4;  $N=4$ ). EMG activity ended  $14 \pm 6$  ms prior to the timing of peak force, which was  $112.5 \pm 25.9$  N ( $N=4$ ) and occurred  $50 \pm 3$  ms after the onset of muscle shortening (Figs 3, 4; Table 2). As during level flight, force production ended just prior to the end of the downstroke (Figs 3, 4).

#### Mechanical work and power output

Plotting force *versus* length for the wingbeat cycles of mallards 2 and 3 shown in Fig. 3 gives the *in vivo* work loops generated by the pectoralis muscles of these two birds (Fig. 5). These represent the extremes of the force/length patterns we observed for the four birds in this study. In general, individual differences in work loop shape resulted mainly from variation in the pattern of force that was calibrated from DPC strain and, to a much lesser extent, changes in the timing of length change relative to force development. As shown in Fig. 5, patterns of work loop shape within an individual animal were generally similar for both flight behaviors. Patterns of *in vivo* fascicle length change were highly consistent across both individuals and flight behaviors. Although the variations in force

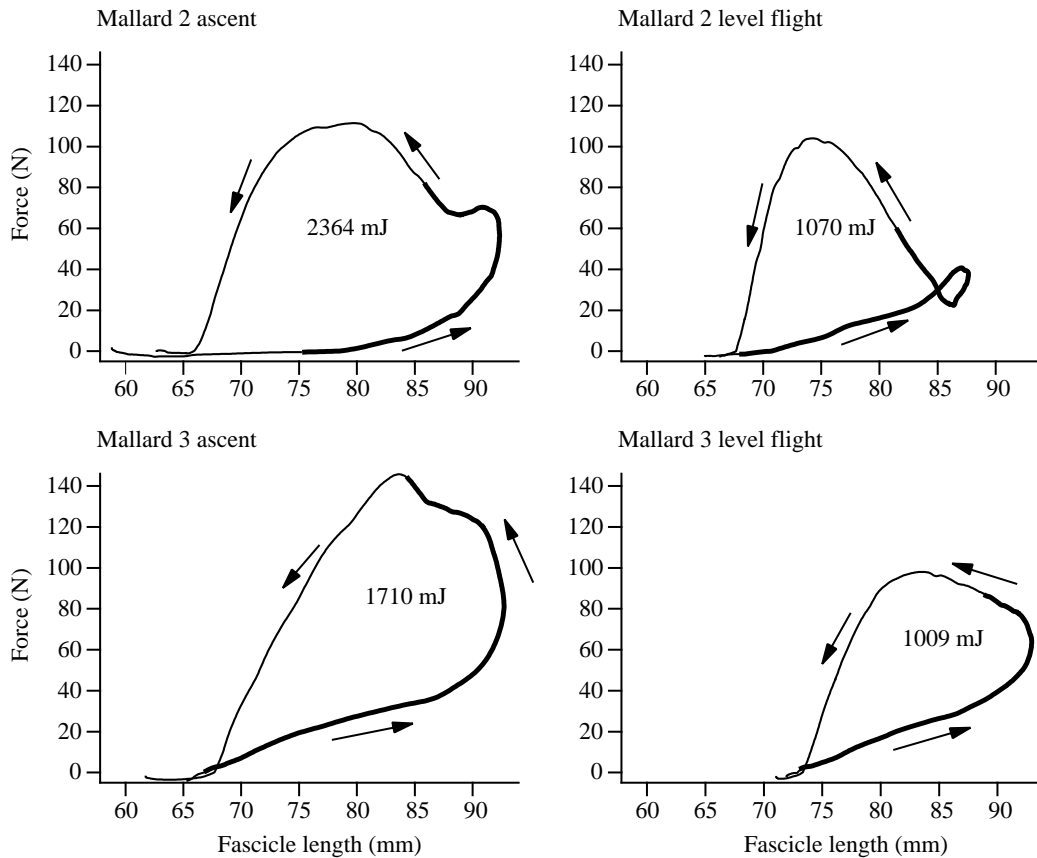


Fig. 5. Work loops calculated directly from the force/length traces in Fig. 3. The area within the loops is equal to the net work done in the cycle. The arrows show the counterclockwise direction of progression of the loop. The bold portions of the lines indicate electromyographic activity.

development resulted in differences in the appearance of work loops between individuals, the general patterns of force/length behavior and the calculated work and power output were consistent across individuals (see below).

The area within each work loop represents the net work done by the muscle during the cycle. The small loop at maximum length in the work loop for mallard 2 results from the drop in force following the upstroke/downstroke transition which, as we noted above, is probably an artifact of gauge misalignment. Mean net work per cycle ranged from  $1312 \pm 248$  mJ ( $N=4$ ) during ascent to  $1004 \pm 172$  mJ ( $N=4$ ) during level flight (Table 2). Multiplying by wingbeat frequency gives an average mechanical power output of the pectoralis over an entire wingbeat cycle of  $11.6 \pm 1.8$  W during ascending flight and  $8.4 \pm 1.5$  W during slow level flight. Accounting for both pectoralis muscles, therefore, gives a total mechanical power output of 23.2 W during ascent and 17.0 W during slow level flight (Table 2). These values correspond to a muscle-mass-specific power output of  $174.2 \pm 31.2$  W kg<sup>-1</sup> during ascent and  $130.9 \pm 47.7$  W kg<sup>-1</sup> during level flight and to a body-mass-specific power of  $23.3 \pm 3.8$  and  $17.0 \pm 2.6$  W kg<sup>-1</sup>, respectively (Table 2). Whole-body climbing power calculated from video recordings of the ascending flight sequences used for *in vivo* analyses was  $17.5 \pm 2.6$  W ( $N=3$ ) compared with the pectoralis power of  $23.2 \pm 3.5$  W measured

*in vivo* over the same intervals. Whole-body power during presurgical flight recordings of ascending flight was  $17.6 \pm 3.3$  W ( $N=3$ ), indicating that flight performance was not hindered by the surgical procedure or by the additional drag from the cable and implanted instruments.

## Discussion

### *Pectoralis force/length behavior*

A central goal of this study was to characterize *in vivo* pectoralis force/length behavior in mallards with respect to mechanical work and power output and to compare this for two differing modes of flight. A second goal was to compare these measurements with similar measurements obtained previously for pigeons during slow level flight. Our results indicate that the general pattern of pectoralis force/length behavior during flight in mallards is similar to that observed in pigeons. However, the contractile dynamics of the mallard pectoralis demonstrate several features that may serve to augment force and mechanical power produced over the course of the wingbeat cycle.

The length trajectory observed in the mallard pectoralis was consistently asymmetrical, with the shortening phase occupying approximately two-thirds of the cycle in both flight modes. This is similar to the pattern of pectoralis length change recorded in

silver king pigeons, in which shortening made up 63% of the cycle period during slow level flight (Biewener et al., 1998). Such an asymmetry has been shown to enhance power production in cyclical contractions *in vitro* (Askew and Marsh, 1997). By increasing shortening duration, a muscle can achieve a larger strain at a given cycle frequency, which may allow it to contract at a shortening velocity that optimizes its power output. Consistent with this interpretation, the shortening strain of the mallard pectoralis was large (29% during slow level flight, 36% during ascent) and similar to the amplitude of strain observed previously in the pigeon (32% during slow level flight; Biewener et al., 1998). However, confirmation that the muscle's *in vivo* shortening velocity and strain pattern maximize power output will require *in vitro* or *in situ* measurements showing that the force/velocity properties and power characteristics of avian pectoralis fibers match the patterns observed for mouse muscle fibers (Askew and Marsh, 1997).

Earlier studies have also suggested that a longer shortening phase may favor increased power output by providing a longer period of activation to enhance force development (Askew and Marsh, 1997; Josephson, 1985). Consistent with this, we found that EMG duration occupied a slightly greater (though not significant) fraction of the wingbeat cycle during ascent, which presumably requires higher force and power output compared with slow level flight. In both flight modes, the timing and duration of neural activation enabled the pectoralis to generate force throughout all but the last 2–3 ms of the shortening phase (Figs 3, 4). Finally, an extended shortening phase (at a given frequency) requires an abbreviated lengthening phase, necessitating a higher velocity of muscle stretch. Increased stretch velocity has been shown to increase the rate of force development when a muscle is actively lengthened (Askew and Marsh, 1997; Edman et al., 1978). Consequently, this suggests that the distinct and prolonged period of active lengthening may represent a third factor important to the force development and power output of the mallard pectoralis.

The peak forces that we recorded from the mallard pectoralis during flight indicate high intramuscular stresses. Mean peak myofibrillar stresses (calculated from mean muscle force/mean muscle area) of 236 kPa during ascending flight and 226 kPa during level flight were far greater than those previously reported for starlings (122 kPa; Biewener et al., 1992) and pigeons (77 kPa; Dial and Biewener, 1993). The greater pectoralis stress observed in mallards may reflect, in part, the muscle's smaller size compared with that of pigeons (13.6% of body mass *versus* 20.0% in pigeons; Dial and Biewener, 1993) and the mallard's greater wing loading (see below). When normalized to body mass<sup>2/3</sup> (assuming isometry), myofibrillar area – a better measure of a muscle's force-generating ability – is also much lower in mallards (0.20) than in pigeons (0.34). However, this is not the case for starlings, which have a comparably sized pectoralis [15% of body mass and an area/(body mass)<sup>2/3</sup> ratio of 0.20], but generate 50% lower stresses during flight. It therefore also seems likely that the greater stresses within the mallard pectoralis may reflect greater recruitment of the muscle's motor unit population

under comparable conditions of performance. However, our data do not allow us to test this possibility.

Finally, as noted above, force development is also probably augmented by the prolonged stretch of the muscle and strain energy released in elastic elements when the muscle begins to shorten. Active lengthening of the mallard pectoralis, however, is so large (on average, approximately 10% of resting length) that it must require the detachment and re-attachment of cross-bridges over several cycles. While this may limit the extent to which active stretch can enhance force development, evidence exists that force enhancement can be achieved even when stretch occurs at longer lengths where the overlap between the thick and thin filaments is decreased (Edman et al., 1978). Previous studies have also suggested that a muscle's ability to develop force under dynamic conditions can exceed what would be expected from its standard force/velocity properties (Franklin and Johnston, 1997; Stevens, 1993). Although the exact mechanism for this is unknown, it is suspected that active lengthening of the muscle is a contributing factor (Franklin and Johnston, 1997).

Although our measurements indicate that significant negative work is done against the mallard pectoralis during the upstroke, the increased force and power output that probably result from its active lengthening would appear to augment considerably the net work and power achieved over an entire wingbeat cycle. The maximal muscle-mass-specific power reported here (174 W kg<sup>-1</sup>) exceeds that estimated for pigeons (119 W kg<sup>-1</sup>; Dial and Biewener, 1993) and matches the highest muscle-mass-specific induced power obtained on the basis of the maximum load-lifting capacity of flying animals (111–177 W kg<sup>-1</sup>; Marden, 1987). The high muscle-mass-specific power output of the mallard pectoralis is consistent with its relatively small size and high operating stress. Previous studies (Marden, 1987; Marden, 1994) suggest that a pectoralis as small as that of the mallards in this study (13.6% of body mass), given similarly proportioned supracoracoideus and distal wing muscles, would be indicative of marginal flight capability. However, the birds in this study were clearly capable of explosive, near-vertical take-off and ascent. Hence, their burst flight capacity may well reflect power augmentation resulting from greater muscle recruitment and force enhancement due to active lengthening during the upstroke.

#### *Effect of flight mode on pectoralis and whole-body performance*

Because of the need for potential energy gain, the mechanical requirements of ascending flight are expected to exceed those of slow level flight. We hypothesized that this increased power demand would be met by similarly matched increases in the magnitudes of pectoralis muscle force, cycle frequency and fascicle length change. However, we found that the higher power requirements of ascending flight were met mainly by an increase in pectoralis muscle strain (from 0.29 to 0.36; a 24% increase), with a smaller increases in force (from 107 to 113 N, a 6% increase) and wingbeat frequency (from 8.4 to 8.9 Hz, a 6% increase). [N.B. Due to the relatively small

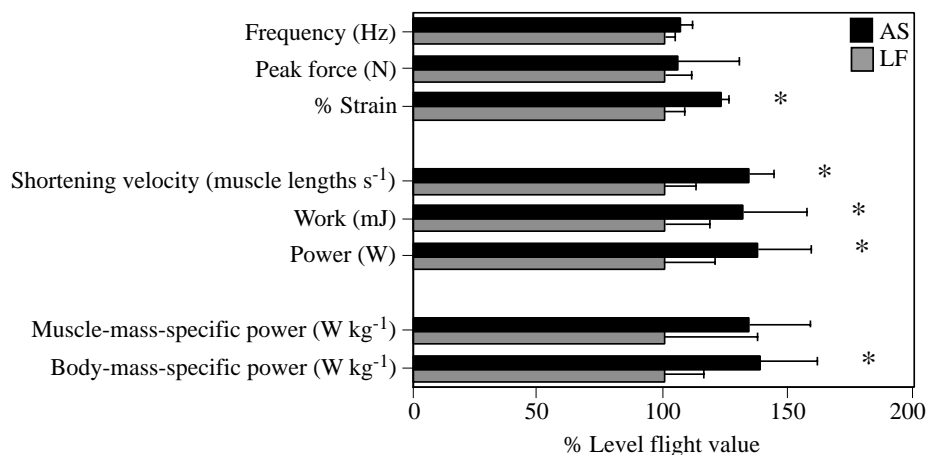


Fig. 6. Histogram showing a comparison of pectoralis performance during ascending (AS) and level (LF) flight. All values (means + s.d.) for a given variable are presented as a percentage of the mean level flight value for that variable. An asterisk denotes a significant difference between ascending and level flight ( $P < 0.05$ ).

sample size ( $n=4$ ), none of these differences are statistically significant.] As a result, significant increases in shortening velocity, muscle work, total muscle power and body-mass-specific power (with an upward trend in muscle-mass-specific power) were observed during ascending flight (Table 2; Fig. 6). Because any increase in shortening velocity to increase power reduces the ability of a muscle to generate force, the potential for increasing power through greater force production in combination with greater strain and frequency may be limited. The high myofibrillar stress observed during slow level flight (226 kPa) also indicates substantial muscle recruitment for this level of performance, suggesting that the margin for additional recruitment to increase force for ascending flight may be rather small. The limited increase in frequency suggests that the mallard pectoralis may operate at a contractile frequency that approaches an optimum for power generation at the length trajectory used (Askew and Marsh, 1997). This is supported by the observation that the relative timing of activation, force development and fascicle length change generally remained the same for both flight modes (Fig. 4), leading to consistent work loop shape across flight mode for each individual (Fig. 5).

Kinematic analysis of the movement of the center of mass during the ascent phase revealed a mean whole-body climbing power of 17.5 W, compared with the 23.2 W obtained from the *in vivo* measurements for the same flight sequences. This suggests that the power requirement of climbing flight is probably not a simple linear sum of the power required for level flight and the rate of potential energy gain. Otherwise, the expected mechanical power output during ascent would be as high as 34.5 W (17.0 W for level flight power plus 17.5 W climbing power) instead of the 23.2 W we report here. One possible explanation for this discrepancy is that other wing muscles (e.g. supracoracoideus) may contribute useful aerodynamic power during ascent, which our pectoralis measurements ignore. However, given that the pectoralis is considerably larger than the supracoracoideus and all other forelimb muscles combined, and that it can power level flight when active alone (Dial, 1992), we believe that the power contribution of the other wing muscles is probably a fairly

small fraction of that produced by the pectoralis. Another possibility is that one or more components of aerodynamic power (e.g. induced power) may be substantially lower during a climb than during slow level flight. However, we are unaware of published evidence, particularly for avian flapping flight, which shows this to be the case. Finally, we suggest that the discrepancy between whole-body power relative to pectoralis muscle power may reflect the use of non-steady mechanisms for lift generation that allow a more efficient translation of muscle mechanical power into useful aerodynamic power during the climbing flight of mallards. Such non-steady effects have been shown to be important in insect flight (e.g. Dickinson et al., 1999; Willmott and Ellington, 1997; Weis-Fogh, 1973) and, we believe, may also be important during flight in birds. Future studies of avian wing kinematics in relation to airflow over the wings would be of considerable value in evaluating this possibility.

#### *Pectoralis performance in mallards versus pigeons*

The silver king pigeons (*Columbia livia*) used in a similar study of *in vivo* pectoralis performance (Biewener et al., 1998) are selectively bred, large racing pigeons. Despite having a 50% greater body mass than that of silver king pigeons, the mallards studied here had only a 16% greater pectoralis mass. In addition, the mallards had a 42% greater wing loading (body weight per unit wing area) than the silver king pigeons. Therefore, the mallards had both smaller pectoralis muscles and smaller wings than the pigeons for their size (Fig. 7; Table 3), suggesting a greater muscle power requirement to achieve a given amount of body-mass-specific aerodynamic power.

The morphology of the DPC also differs somewhat between these two species in that the mallards have a relatively longer and less pronounced DPC. Although this probably introduces some variation in the principal strains developed within the DPC of mallards compared with pigeons, the general patterns of principal tensile strain resulting from pectoralis activity are quite similar. In both species, the principal strain orientation varies over a similar range during the downstroke and is nearly perpendicular to the longitudinal axis of the humeral shaft at

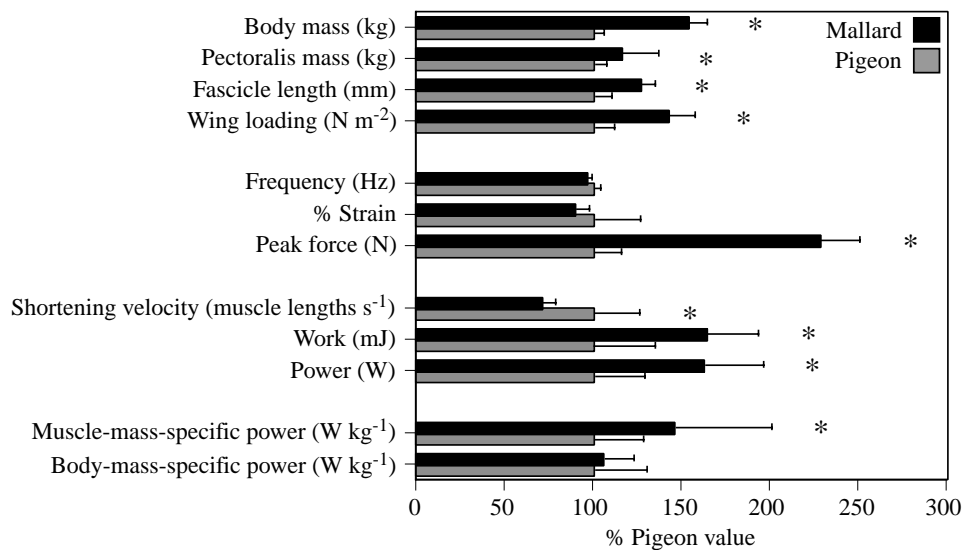


Fig. 7. Histogram showing a comparison of mallard and pigeon morphology and a comparison of pectoralis performance during slow level flight. All values (means + s.d.) for a given variable are presented as a percentage of the mean pigeon value for that variable. An asterisk denotes a significant difference between mallard and pigeon ( $P < 0.05$ ) (pigeon values are taken from Biewener et al., 1998).

peak strain (compare Fig. 1 here with Fig. 1 in Dial and Biewener, 1993). The similarity in principal strain pattern suggests that morphological differences in the DPC between the two species have only a modest effect on pectoralis force measurements derived from DPC strain, given appropriate strain gauge alignment.

A comparison of the pectoralis performance of the mallards and pigeons during slow level flight (Fig. 7) reveals that wingbeat frequency and pectoralis fascicle strain are similar for both species, with the pigeons exhibiting slightly higher mean values for both variables. As a result, the pigeon pectoralis achieves a significantly greater shortening velocity than that of the mallard. However, because the magnitude of pectoralis force generated by the mallards was far greater (2.3 times) than that of the pigeons, pectoralis work, power and muscle-mass-specific power are all significantly greater in the mallards. Nevertheless, because of the relatively smaller size of the mallard pectoralis and their slightly lower wingbeat frequency and muscle strain, whole-body mass-specific power is nearly equivalent in these two species during slow level flight (Fig. 7), consistent with the classical aerodynamic prediction of size-independent mass-specific power requirement for flight (Ellington, 1991).

The difference in pectoralis force output for these two species may be largely explained, therefore, by the greater body mass and greater wing loading of the mallards, which require them to generate greater muscle forces to achieve equivalent mass-specific aerodynamic pressure. Another possibility, suggested by their relatively shorter, more rounded wings compared with the higher-aspect-ratio wings of mallards, is that the pigeon pectoralis may have a greater mechanical advantage for generating aerodynamic force. Because of the uncertainties of defining the likely time-varying location of the center of aerodynamic pressure acting on the wing during flapping flight, confirmation of this hypothesis is not possible. However, using the center of area of the extended wing as an approximation of the center of pressure on the wing

during the downstroke, our calculations of the mechanical advantage of the wing in mallards compared with that of white carneau pigeons yield nearly identical values: 0.100 and 0.099, respectively ( $N=2$  for each). Although this approach is oversimplified, it nevertheless suggests that mechanical advantage is unlikely to be a major factor underlying the observed differences in the magnitude of force generation between these two species.

The higher force requirement of the mallard pectoralis is probably met by a combination of greater motor recruitment and enhancement of the force generated by activated fibers resulting from their being actively lengthened. Although this pattern of active lengthening is prominent in the mallard, it is far less evident in the contractile dynamics of the pigeon pectoralis. Direct recordings of fascicle length change and force in the pigeon pectoralis (Biewener et al., 1998) demonstrated only modest active lengthening, with force developing over a narrower range of fascicle length about the upstroke/downstroke transition. The size and morphology of the pigeon apparently allow it to achieve sufficient mass-specific power for slow level flight without incurring the high myofibrillar stress observed in the mallard, suggesting that pigeons may have a greater capacity for increasing power and overall flight performance. This is supported by the fact that wild-type pigeons can achieve a greater body-mass-specific climbing power ( $26.4 \text{ W kg}^{-1}$ ; Dial and Biewener, 1993) than the  $17.5 \text{ W kg}^{-1}$  found here for mallards.

The relatively small pectoralis and long, high-aspect-ratio wings of the mallards may adapt them to high-speed, long-distance migratory flight, for which aerodynamic power requirements are minimal. However, these characteristics may also limit their capacity for low-speed and maneuvering flight, particularly in comparison with pigeons and other smaller, more agile species. It will be interesting to examine mechanical power performance in other anseriform birds of various sizes (e.g. teal, geese and swans) to determine whether these birds exhibit a similar pattern of constraint on

slow-speed maneuvering flight in favor of high-speed, long-distance flight performance and how this relates to their behavioral ecology.

The authors wish to thank Pedro Ramirez for assistance in caring for the birds, Bret Tobalske for advice on the analysis and Peter Weyand, Gary Gillis and Matt Bundle for helpful comments on an earlier draft of the manuscript. This work was supported by NSF grants IBN-9823699 (A.A.B.) and IBN-9507503 (K.P.D.).

### References

- Askew, G. N. and Marsh, R. L.** (1997). The effects of length trajectory on the mechanical power output of mouse skeletal muscles. *J. Exp. Biol.* **200**, 3119–3131.
- Biewener, A. A., Corning, W. R. and Tobalske, B. W.** (1998). *In vivo* pectoralis muscle force/length behavior during level flight in pigeons (*Columbia livia*). *J. Exp. Biol.* **201**, 3293–3307.
- Biewener, A. A., Dial, K. P. and Goslow, G. E., Jr** (1992). Pectoralis muscle force and power output during flight in the starling. *J. Exp. Biol.* **164**, 1–18.
- Calow, L. J. and Alexander, R. McN.** (1973). A mechanical analysis of the hind leg of a frog (*Rana temporaria*). *J. Zool., Lond.* **171**, 293–321.
- Dial, K. P.** (1992). Avian forelimb muscles and nonsteady flight: can birds fly without using the muscles of their wings? *Auk* **109**, 874–885.
- Dial, K. P. and Biewener, A. A.** (1993). Pectoralis muscle force and power output during different modes of flight in pigeons (*Columbia livia*). *J. Exp. Biol.* **176**, 31–54.
- Dial, K. P., Biewener, A. A., Tobalske, B. W. and Warrick, D. R.** (1997). Mechanical power output of bird flight. *Nature* **390**, 67–70.
- Dickinson, M. H., Lehmann, F. O. and Sane, S. P.** (1999). Wing rotation and the aerodynamic basis of insect flight. *Science* **284**, 1954–1960.
- Edman, K. A. P., Elzinga, G. and Noble, M. I. M.** (1978). Enhancement of mechanical performance by stretch during tetanic contractions of vertebrate skeletal muscle fibres. *J. Physiol., Lond.* **281**, 139–155.
- Ellington, C. P.** (1991). Limitations on animal flight performance. *J. Exp. Biol.* **160**, 71–91.
- Franklin, C. E. and Johnston, I. A.** (1997). Muscle power output during escape responses in an Antarctic fish. *J. Exp. Biol.* **200**, 703–712.
- Goldman, D. E. and Heuter, T. F.** (1956). Tabular data of the velocity and absorption of high frequency sound in mammalian tissues. *J. Acoust. Soc. Am.* **28**, 35–53.
- Griffiths, R. I.** (1987). Ultrasound transit time gives direct measurement of muscle fiber length *in vivo*. *J. Neurosci. Meth.* **21**, 159–165.
- Josephson, R. K.** (1985). Mechanical power output from striated muscle during cyclical contraction. *J. Exp. Biol.* **114**, 493–512.
- Marden, J. H.** (1987). Maximum lift production during takeoff in flying animals. *J. Exp. Biol.* **130**, 235–258.
- Marden, J. H.** (1994). From damselflies to pterosaurs: how burst and sustainable flight performance scale with size. *Am. J. Physiol.* **266**, R1077–R1084.
- Marsh, R. L., Olson, J. M. and Guzik, S. K.** (1992). Mechanical performance of scallop adductor muscle during swimming. *Nature* **357**, 411–413.
- Norberg, U. M.** (1990). *Vertebrate Flight: Mechanics, Physiology, Morphology, Ecology and Evolution*. Heidelberg: Springer-Verlag.
- Pennycuik, C. J.** (1968). Power requirements for horizontal flight in the pigeon *Columbia livia*. *J. Exp. Biol.* **49**, 527–555.
- Pennycuik, C. J.** (1989). *Bird Flight Performance: A Practical Calculation Manual*. Oxford: Oxford University Press.
- Pennycuik, C. J., Hedenstrom, A. and Rosen, M.** (2000). Horizontal flight of a swallow (*Hirundo rustica*) observed in a wind tunnel, with a new method for directly measuring mechanical power. *J. Exp. Biol.* **203**, 1755–1765.
- Rayner, J. M. V.** (1979). A new approach to animal flight mechanics. *J. Exp. Biol.* **80**, 17–54.
- Rosser, B. W. C. and George, J. C.** (1986). The avian pectoralis: histochemical characterization and distribution of muscle fiber types. *Can. J. Zool.* **64**, 1174–1185.
- Spedding, G. R.** (1986). The wake of a jackdaw (*Corvus monedula*) in slow flight. *J. Exp. Biol.* **125**, 287–307.
- Spedding, G. R., Rayner, J. M. V. and Pennycuik, C. J.** (1984). Momentum and energy in the wake of a pigeon (*Columbia livia*) in slow flight. *J. Exp. Biol.* **111**, 81–102.
- Stevens, E. D.** (1993). Relation between work and power calculated from force–velocity curves, to that done during oscillatory work. *J. Muscle Res. Cell Motil.* **14**, 518–526.
- Weis-Fogh, T.** (1973). Quick estimates of flight fitness in hovering animals, including novel mechanisms for lift production. *J. Exp. Biol.* **59**, 169–230.
- Weis-Fogh, T. and Alexander, R. McN.** (1977). The sustained power output from striated muscle. In *Scale Effects of Animal Locomotion* (ed. T. J. Pedley), pp. 511–525. London: Academic Press.
- Willmott, A. P. and Ellington, C. P.** (1997). The mechanics of flight in the hawkmoth *Manduca sexta*. II. Aerodynamic consequences of kinematic and morphological variation. *J. Exp. Biol.* **200**, 2723–2745.